

Brillouin amplification supports 1×10^{-20} uncertainty in optical frequency transfer over 1400 km of underground fiber

Sebastian M. F. Raupach,^{*} Andreas Koczwara, and Gesine Grosche

Physikalisch-Technische Bundesanstalt (PTB), Bundesallee 100, D-38116 Braunschweig, Germany

(Received 20 March 2015; published 24 August 2015)

We investigate optical frequency transfer over a 1400 km loop of underground fiber connecting Braunschweig and Strasbourg. Largely autonomous fiber Brillouin amplifiers are the only means of intermediate amplification used here. This allows phase-continuous measurements over periods up to several days. Over a measurement period of about three weeks we find a weighted mean of the transferred frequency's fractional offset of $(1.1 \pm 0.4) \times 10^{-20}$. In the best case we find an instability of 6.9×10^{-21} and a fractional frequency offset of 4.4×10^{-21} at an averaging time of around 30 000 s. These results represent an upper limit for the uncertainty over 1400 km when using a chain of remote Brillouin amplifiers, and allow one to compare the world's best optical clocks.

DOI: [10.1103/PhysRevA.92.021801](https://doi.org/10.1103/PhysRevA.92.021801)

PACS number(s): 42.60.Da, 06.30.Ft, 06.20.fb

The transfer of optical frequencies [1–6] is required, e.g., for comparing the ultrastable signals generated by optical frequency standards. For such standards record uncertainties at the 10^{-18} level were reported recently [7–9]. Transferring their ultrastable optical output is required for their operation as clocks contributing to a universal time scale, for independent validation via remote comparison, and for applications such as relativistic geodesy [10–12]. Optical frequency transfer can also serve to disseminate an optical reference to remote users [6,13]. Taking advantage of phase synchronicity at the sending and receiving end [14], it can be used for common-mode suppression of the Dick effect in optical clock comparisons via synchronous sampling [8,15,16]. The noise added by the transmission path can be minimized using underground fiber links, and by actively stabilizing the phase of the transferred signal [2,3,5]. Alternatively the two-way technique may be employed [17–19]. In view of clock uncertainties close to 1×10^{-18} , hitherto demonstrated uncertainty contributions of long-distance optical frequency transfer of $2\text{--}5 \times 10^{-19}$ [2–5] can no longer be neglected.

In long-distance links the losses in silica telecommunication fiber are traditionally compensated by broadband erbium doped fiber amplifiers (EDFA). For ultrastable optical frequency transfer they have to be operated without isolators to ensure symmetry of the optical path in both directions [20,21]. This makes them sensitive to backscatter and back reflection, leading to significant amplitude variations and signal outages. Thus the gain is restricted to about 15 dB [22], resulting in excess losses over long distances. In long-distance, bidirectional EDFA links the signal phase may be lost at least several times per hour [4,5]. Very recently, for a 540 km loop of cascaded, phase-stabilized EDFA links an instability (as estimated by the modified Allan deviation) of 3×10^{-20} was reported [19]; an accuracy was not reported.

Narrow-band fiber Brillouin amplification in the field [6,21] is an alternative approach being investigated after early demonstrations of Brillouin-assisted frequency transfer [3,23]. Promising results were obtained with a single, in-the-field fiber Brillouin amplifier (FBA), where frequency transfer on the 10^{-19} level was demonstrated [6]. The scalability of this

approach by cascading autonomous field systems is not clear, and its phase noise contributions to optical frequency transfer are not known.

In this Rapid Communication we present a single span 1400 km fiber link (attenuation > 300 dB) from Braunschweig (Germany) to Strasbourg (France) and back, which relies solely on cascaded, fieldable FBA for intermediate amplification. This link also forms part of the international optical metrology link PTB (Germany)/LNE-SYRTE (France).

Employing cascaded Brillouin amplification, we demonstrate the transfer of an optical frequency over this continental-scale distance with an uncertainty $< 2 \times 10^{-20}$. We constrain uncertainty contributions due to the cascade of FBA to below 10^{-20} . We find that cascaded Brillouin amplification in the field allows phase-continuous, amplitude-stable measurements over periods up to several days. We demonstrate that an optimized data analysis allows remote comparisons of the world's best optical frequency standards over this distance; here they would be dominated by the clock noise already from 10 s onwards. Our results indicate the scalability of this approach up to the longest continental distances paving the way for large scale relativistic geodetic measurements and the realization of a universal optical time scale.

The fiber link consists of a pair of telecommunication fibers connecting PTB in Braunschweig to Université de Strasbourg (UDS) over a fiber length of around 710 km. The fibers are patched together at UDS to form a loop starting and ending in the same laboratory at PTB to facilitate the characterization of the link. For active phase stabilization, the link is set up as a fiber Michelson interferometer as in [3,6]. As a frequency source for the transfer, we use a laser at 194.4 THz locked to a cavity-stabilized 1 Hz master laser. For a clock comparison the transfer laser might be measured against, or locked to, the clock laser. We use bidirectional EDFA as booster amplifiers for the outgoing and the incoming light. The local, stabilization interferometer and the setup for detecting the “remote” beat frequency between the transferred and the source light are located in separate but adjacent, thermally insulated housings (see Fig. 1). Beat frequencies are recorded using K&K FXE dead-time-free totalizing counters with an internal gate time of 1 ms [3,5,13,18,24]. The counters are set to report the frequency values at 1 s intervals, both as equally weighted frequency averages (“IT” mode [25]) and as

^{*}sebastian.raupach@ptb.de

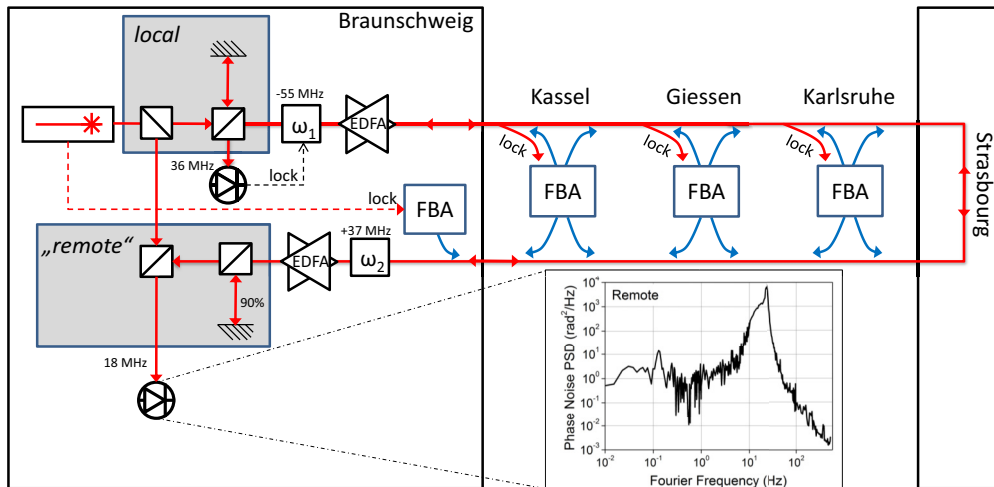


FIG. 1. (Color online) Schematic sketch of the all-fiber measurement setup and the 1400 km Brillouin link PTB-Universität de Strasbourg-PTB. The inset shows the remote beat phase noise, calculated from 1 ms phase data (K&K-FXE).

triangularly weighted, overlapping frequency averages (“ Λ ” mode [25]) implemented by averaging the phase values. The averaging strongly suppresses phase fluctuations with Fourier frequencies larger than the reciprocal of the report interval (see [25,26] for a related discussion). The overall measurement setup at PTB is described in more detail in [6].

Along the link we have installed three fieldable FBA in server rooms of Kassel University, Giessen University, and the Karlsruhe Institute of Technology. The remote (Fig. 1) signal experiences seven Brillouin amplifications, corresponding to an average interamplifier distance of 200 km. The individual lengths bridged and their attenuations are 205 km/44 dB (Braunschweig-Kassel), 160 km/33 dB (Kassel-Giessen), 231 km/47 dB (Giessen-Karlsruhe), and around 2×114 km/54 dB (Karlsruhe-Strasbourg-Karlsruhe), respectively. The first fiber stretch has been shortened slightly since earlier measurements [6].

Each FBA contains one pump laser, the light of which is split into four paths. It serves two fibers simultaneously by injecting about 10 mW of pump light in each direction. In two of the paths the pump light’s frequency is shifted by an acousto-optic modulator to accommodate the frequency shift of 74 MHz of the signal returning from the remote end. The frequency of the pump laser is locked to the incoming, amplified signal at an offset frequency of around 11 GHz, corresponding to the fiber’s Brillouin frequency. The FBA allow remote locking as well as remote optimization of the pump laser lock and polarization. However, usually they run autonomously, as is the case for the measurements presented here. Even without polarization adjustment, all FBA stay in lock at least several days.

We have performed two measurement campaigns from December 10, 2014 to December 18, 2014, and from December 23, 2014 to January 2, 2015. During the first campaign we observed average failure rates of about four outliers per day; during the second campaign the stabilization of the link failed within five 1-s intervals only, indicated by five outliers in the remote and in-loop beat frequency. This demonstrates a high overall reliability and very low cycle slip rate. The signal-to-noise ratio of the beat frequencies is around 30 dB

(100 kHz bandwidth), and short-term amplitude fluctuations are < 1 dB.

To assess the accuracy of the optical frequency transfer we calculate the arithmetic mean of the difference between the expected and the measured beat frequency at the remote end.

Results for optical frequency transfer over the 1400 km are shown in Fig. 2. The filled circles illustrate the instability (Allan deviation, ADEV [27]) of equally weighted averages of Π data [25] (bandwidth > 10 kHz); it falls off with the averaging time τ as $1/\tau$. We find an unweighted mean of the transfer-induced frequency offset of 2.7×10^{-19} , below the instability of 1.5×10^{-18} indicated by the last value of the Allan deviation. The dashed line in Fig. 2 indicates the instability of the most recent side-by-side or self-comparison of optical clocks [8,9]: using full-bandwidth Π -type data would obscure their performance up to the longest averaging times. But such a large bandwidth is not required: in optical frequency standards the atomic reference typically contributes information only over times larger than a few seconds, corresponding to a bandwidth < 1 Hz (typically < 0.1 Hz).

We now adjust our data processing accordingly, by applying the Allan deviation to the Λ data (phase averaged data). The phase averaging is similar to applying a sinc-shaped “low-pass filter” to the phase fluctuations; the sinc’s first zero corresponds to the inverse of the indicated gate time τ (1 Hz in Fig. 2; see also [25,28]). We add a prefix “ Λ ” to specify the filter. This filtering here reduces the instability (at 1 s) by a factor of 75, while the slope of $1/\tau$ remains unchanged. For averaging times larger than about 100 s, even the best optical clocks would now dominate the instability of the frequency transferred over 1400 km. We find an instability (Λ_{1s} -ADEV) at an averaging time $\tau \approx 97\,000$ s of 1.9×10^{-20} , and an unweighted mean of the Λ data of 1.0×10^{-20} (total, continuous measurement time here around 390 000 s, corresponding to more than four days).

Also shown are the modified Allan deviations (ModADEV [25,27]) of the remote and in-loop frequencies, as well as that of an example of the relative fluctuations between the local and remote setup.

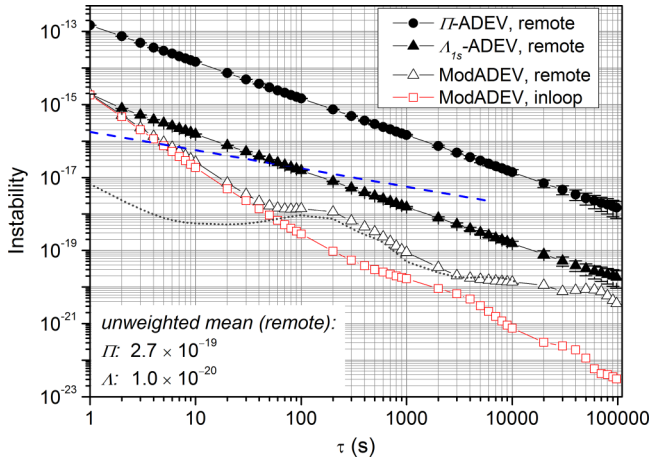


FIG. 2. (Color online) Instability of the optical frequency transfer over the stabilized 1400 km “Brillouin link” Braunschweig-Strasbourg-Braunschweig. The frequency data are reported once per second simultaneously in Π and in Λ mode (FXE K&K); filled circles: Allan deviation of the frequency transfer (Π -type data, bandwidth > 10 kHz); filled triangles: Allan deviation of Λ -type remote frequency offset data (Λ_{1s} -ADEV, bandwidth 1 Hz); open triangles: modified Allan deviation of the transferred frequency; open squares: modified Allan deviation of the in-loop signal; dashed line: instability of the most recent side-by-side or self-comparisons of optical clocks [8,9]; dotted line: instability without link (“optical shortcut”); the error bars of each ADEV point $\sigma_y(\tau)$ are calculated as $\sigma_y(\tau)/\sqrt{N(\tau)}$ [27], with $N(\tau)$ being the number of averaging intervals at τ .

The modified Allan deviation effectively continues the triangular, overlapping Λ -type averaging for larger intervals τ [25]. It therefore indicates the “starting points” of the Λ_{τ} -ADEV for increasing τ . The ModADEV decreases considerably faster than the ADEV for certain noise types [4,5,13,19]. For continuous measurements we may thus increase the Λ -type averaging interval to exploit this strong decrease in instability. This allows us to obtain a better estimate of the mean frequency (see also [29] for a detailed calculation and discussion).

A different measurement run is shown in Fig. 3, where we furthermore numerically increase the Λ -type averaging to an interval of 10 s (full diamonds), corresponding to a bandwidth of 0.1 Hz. We obtain an unweighted mean of 1.2×10^{-20} and an instability (Λ_{10s} -ADEV) of 1.7×10^{-20} at an averaging time $\tau \approx 36\,000$ s (total, continuous measurement time here around 145 000 s). Here the transfer instability over 1400 km is smaller than that reported for a local clock comparison [8] already for averaging times of 10 s onwards.

Numerically increasing the Λ -averaging interval from 1 to 10 s also for the data shown in Fig. 2 yields an instability (Λ_{10s} -ADEV) at the longest averaging time of 9.9×10^{-21} , and an unweighted mean of 1.2×10^{-20} . These results demonstrate continental-scale optical frequency transfer with an uncertainty $< 2 \times 10^{-20}$.

Figure 4 summarizes the results from all long-term measurements during the measurement period. To search for systematic shifts in the 10^{-20} range, we numerically extend the Λ averaging to 2000 s. The observed residual offsets scatter

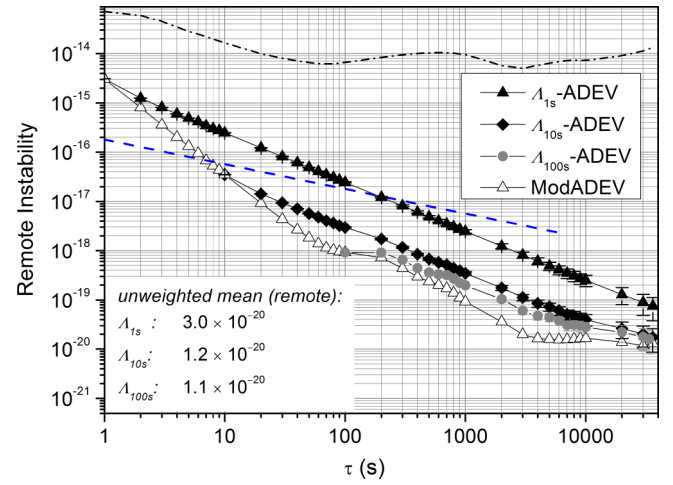


FIG. 3. (Color online) Optical frequency transfer instability (1400 km), different measurement, and demonstration of a numerically extended Λ averaging interval. Filled triangles: Allan deviation of the frequency transfer for Λ -type data phase averaged over 1 s; filled diamonds: $\Lambda_{10s/100s}$ -ADEV of the frequency transfer for Λ -type data, (Λ -type averaging interval: 10 s; gray circles: 100 s); open triangles: modified Allan deviation of the transferred frequency; dashed line: instability of optical clock comparison as in Fig. 2; dash-dotted line: ModADEV of the fiber link stabilization’s correction signal; for frequencies corresponding to the longest averaging time we expect the link stabilization to suppress phase fluctuations by about six orders of magnitude [26].

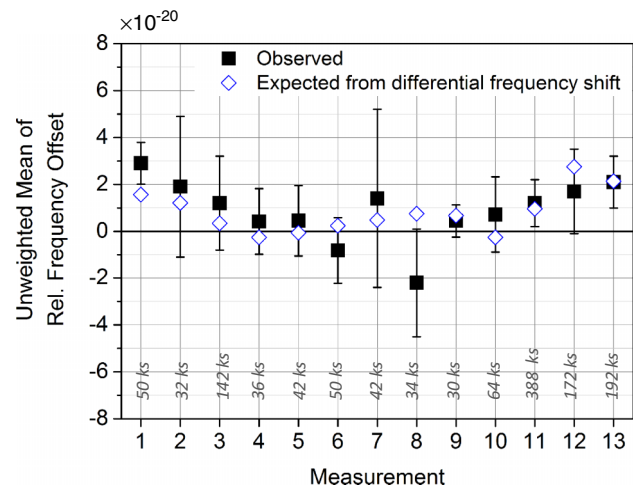


FIG. 4. (Color online) Overview over all long-term measurements during the period from December 10, 2014 to January 2, 2015. The black squares indicate the unweighted means for numerically extended Λ -type averaging intervals of 2000 s; the respective total measurement times are indicated in kiloseconds. The error bars $\pm s$ indicate the last value s of the corresponding Λ_{2000s} -ADEV at 1/4 of the total measurement time, yielding a conservative estimate of the statistical uncertainty [29,30]. The mean of these data weighted by $1/s^2$ is $(1.1 \pm 0.4) \times 10^{-20}$. For comparison, the open diamonds correspond to the unweighted mean of the fiber-induced frequency offset during the respective measurements, multiplied by a factor of $+2 \times 10^{-7}$. This factor corresponds to the relative frequency difference between outgoing and return light.

within $\pm 3 \times 10^{-20}$, and their weighted mean is $(1.1 \pm 0.4) \times 10^{-20}$. In the best case we obtain an instability ($\Delta_{2000\text{s-ADEV}}$) of 6.9×10^{-21} and an unweighted mean of the transferred frequency's offset of 4.4×10^{-21} . We do not observe a significant offset of the in-loop beat frequency, hence the observed offsets most likely indicate out-of-loop processes or nonreciprocal effects along the link, which we consider below.

Due to the 2×37 MHz shift by the remote acousto-optic modulator (AOM), the outgoing light and the returning roundtrip light exhibit a relative frequency difference of 3.8×10^{-7} . To first order, following a dispersion free approximation [31], we thus expect an overcompensation of the frequency offset observed at the remote end by 1.9×10^{-7} as the frequency shift is positive on the return path. These values are shown as open diamonds in Fig. 4. We weakly observe the expected behavior. Other effects that may play a role are the finite suppression of the fiber noise due to the delay limit [26] as well as the relative fluctuations between our separate local and remote interferometers. These are subject to further investigations.

As fiber Brillouin amplification is a novel technique in frequency metrology, we explore fundamental phase noise contributions related to it. Our setup uses a fixed frequency offset between pump and signal to accommodate the Brillouin frequency shift. However, the Brillouin shift depends on the fiber temperature [32]. Hence, temperature changes of the fiber move the Brillouin gain curve relative to the signal frequency. This in turn induces a varying phase shift of the amplified signal, and thus a frequency shift. This is in addition to the well-known symmetric shifts due to changes of the refractive index n in the fiber induced by mechanical and thermal perturbations (see Fig. 3). Here, we are mainly concerned with asymmetric shifts, arising particularly from the remote FBA that amplifies one direction only. As a measure of the temperature variation dT/dt in the fiber we use the frequency deviation of the AOM employed for link stabilization:

$$\Delta v_{\text{link}} = -\frac{1}{2\pi} \frac{d\phi}{dt} \approx -\frac{L}{\lambda} k_n \frac{dT}{dt}, \quad (1)$$

where we neglect the effect of the thermal expansion of the fiber ($\delta L/\delta T$); $k_n = \delta n/\delta T = 1.1 \times 10^{-5}/\text{K}$ [33], fiber length $L = 1.4 \times 10^6$ m. The temperature dependence of the Brillouin frequency is $k_T^B = 1.1$ MHz/K [32]. To investigate the signal phase sensitivity k_ϕ to the Brillouin frequency variation we deliberately modulated the remote FBA pump frequency over a range of about 6 MHz at a rate of several tens of kilohertz per second. We find $k_\phi \approx -4 \times 10^{-7}$ rad/Hz. This yields a scaling factor of

$$\frac{\Delta v_{\text{signal}}^{\text{Brillouin}}}{\Delta v_{\text{link}}} \approx -\frac{k_T^B k_\phi \lambda}{2\pi k_n L} = 8.5 \times 10^{-9}. \quad (2)$$

This effect hence is about eight orders of magnitude smaller than that related to the temperature sensitivity of the fiber's refractive index, which in turn in our measurements is suppressed by about six orders of magnitude (see Fig. 3). It hence is too small to be a limitation here. It could be suppressed further by tracking shifts in the Brillouin frequency. Effects due to the imperfection of the lock are expected to be at least one order of magnitude smaller than the temperature effect. We conservatively estimate the overall effect of the Brillouin amplification on the instability to be smaller than 5×10^{-21} here. This would allow an upscaling to the longest continental distances.

Using a loop consisting of a patched pair of telecommunication fibers connecting Braunschweig to Strasbourg, we have investigated optical frequency transfer over 1400 km of underground fiber in a single span, with a cascade of in-the-field FBA as the sole means of remote amplification. We estimate the effect of cascaded Brillouin amplification on the uncertainty of the transfer to be less than 5×10^{-21} . We have confirmed experimentally that a cascade of Brillouin amplifications supports an uncertainty better than 1×10^{-20} , where the statistical uncertainty is estimated conservatively by the instability [29,34]. Using separately housed local and remote setups, we observe an accuracy of the transferred optical frequency of about $(1.1 \pm 0.4) \times 10^{-20}$.

The results presented here demonstrate frequency transfer at the 10^{-20} uncertainty level over a continental-scale distance; this would allow a relativistic height resolution of around 100 μm . The fiber link supports remote comparisons of the world's best optical clocks over 1400 km, and our analysis and results illustrate the potential for upscaling this approach to the longest continental distances, potentially allowing direct optical clock comparisons between Europe and the Far East.

We thank H. Schnatz and F. Riehle for their long-standing support and are indebted to P.-E. Pottie and colleagues for enabling the cooperation with UDS. S.R. thanks C. Lisdat and E. Benkler for helpful discussions. We are grateful to C. Grebing, and to T. Legero for operating the cavity-stabilized laser. We gratefully acknowledge the support by P. Gris and B. Moya (UDS), O. Bier (ARTE), T. Vetter, H. Klatte, and U. Koc (Kassel University), K. Ackermann (Giessen University), B. Hoelt (K.I.T.), F. Hack, and W.-Ch. König (Gasline GmbH), C. Grimm (Deutsches Forschungsnetz e.V.), E. Camisard (RENATER), and by their colleagues. We thank A. Uhde, H. Brandt, S. Günther, M. Misera, M. Wengel, and J. Falke for excellent technical support. This work is supported by the European Metrology Programme (EMRP) SIB-02 (NEAT-FT). The EMRP is jointly funded by the EMRP participating countries within EURAMET and the European Union.

- [1] O. Lopez, A. Kanj, P.-E. Pottie, D. Rovera, J. Achkar, C. Chardonnet, A. Amy-Klein, and G. Santarelli, *Appl. Phys. B* **110**, 3 (2013).
 [2] O. Lopez, A. Haboucha, B. Chanteau, Ch. Chardonnet, A. Amy-Klein, and G. Santarelli, *Opt. Express* **20**, 23518 (2012).

- [3] K. Predehl, G. Grosche, S. M. F. Raupach, S. Droste, O. Terra, J. Alnis, Th. Legero, T. W. Hänsch, Th. Udem, R. Holzwarth, and H. Schnatz, *Science* **336**, 441 (2012).
 [4] S. Droste, F. Ozimek, Th. Udem, K. Predehl, T. W. Hänsch, H. Schnatz, G. Grosche, and R. Holzwarth, *Phys. Rev. Lett.* **111**, 110801 (2013).

- [5] D. Calonico, E. K. Bertaccho, C. E. Calosso, C. Clivati, G. A. Costanzo, M. Frittelli, A. Godone, A. Mura, N. Poli, D. V. Sutyryn, G. Tino, M. E. Zucco, and F. Levi, *Appl. Phys. B* **117**, 979 (2014).
- [6] S. M. F. Raupach, A. Koczwara, and G. Grosche, *Opt. Express* **22**, 26537 (2014).
- [7] B. J. Bloom, T. L. Nicholson, J. R. Williams, S. L. Campbell, M. Bishof, X. Zhang, W. Zhang, S. L. Bromley, and J. Ye, *Nature (London)* **506**, 71 (2014).
- [8] I. Ushijima, M. Takamoto, M. Das, T. Ohkubo, and H. Katori, *Nat. Photonics* **9**, 185 (2015).
- [9] T. L. Nicholson, S. L. Campbell, R. B. Hutson, G. E. Marti, B. J. Bloom, R. L. McNally, W. Zhang, M. D. Barrett, M. S. Safranov, G. F. Strouse, W. L. Tew, and J. Ye, *Nat. Commun.* **6**, 6896 (2015).
- [10] M. Vermeer, Reports of the Finnish Geodetic Institute **83**, 1 (1983).
- [11] C. W. Chou, D. B. Hume, T. Rosenband, and D. J. Wineland, *Science* **329**, 1630 (2010).
- [12] P. Delva and J. Lodewyck, *Acta Futura* **7**, 67 (2013).
- [13] A. Pape, O. Terra, J. Friebe, M. Riedmann, T. Wübbena, E. M. Rasel, K. Predehl, T. Legero, B. Lipphardt, H. Schnatz, and G. Grosche, *Opt. Express* **18**, 21477 (2010).
- [14] S. M. F. Raupach and G. Grosche, *IEEE Trans. Ultrason. Ferroelectr. Freq. Control* **61**, 920 (2014).
- [15] M. Takamoto, T. Takano, and H. Katori, *Nat. Photonics* **5**, 288 (2011).
- [16] T. Akatsuka, H. Ono, K. Hayashida, K. Araki, M. Takamoto, T. Takano, and H. Katori, *Jpn. J. Appl. Phys.* **53**, 032801 (2014).
- [17] C. E. Calosso, E. Bertacco, D. Calonico, C. Clivati, G. A. Costanzo, M. Frittelli, F. Levi, A. Mura, and A. Godone, *Opt. Lett.* **39**, 1177 (2014).
- [18] A. Bercy, F. Stefani, O. Lopez, C. Chardonnet, P.-E. Pottie, and Anne Amy-Klein, *Phys. Rev. A* **90**, 061802(R) (2014).
- [19] F. Stefani, O. Lopez, A. Bercy, W.-K. Lee, C. Chardonnet, G. Santarelli, P.-E. Pottie, and A. Amy-Klein, *J. Opt. Soc. Am. B* **32**, 787 (2015).
- [20] Ł. Sliwczynski and J. Kołodziej, *IEEE Trans. Instrum. Meas.* **62**, 253 (2013).
- [21] S. M. F. Raupach, A. Koczwara, G. Grosche, F. Stefani, O. Lopez, A. Amy-Klein, C. Chardonnet, P.-E. Pottie, and G. Santarelli, Proceedings of the 2013 Joint IEEE International Frequency Control Symposium and European Frequency and Time Forum, Prague, 2013 (unpublished), p. 883.
- [22] O. Lopez, F. Kéfélian, H. Jiang, A. Haboucha, A. Bercy, F. Stefani, B. Chanteau, A. Kanj, D. Rovera, J. Achkar, C. Chardonnet, P.-E. Pottie, A. Amy-Klein, and G. Santarelli, *C. R. Phys.* **16**, 531 (2015).
- [23] O. Terra, G. Grosche, and H. Schnatz, *Opt. Express* **18**, 16102 (2010).
- [24] G. Kramer and W. Klische, Proceedings of the 18th European Frequency and Time Forum, Guildford, 2004 (unpublished), p. 595, and references therein.
- [25] S. T. Dawkins, J. J. McFerran, and A. N. Luiten, *IEEE Trans. Ultrason. Ferroelectr. Freq. Control* **54**, 918 (2007).
- [26] P. A. Williams, W. C. Swann, and N. R. Newbury, *J. Opt. Soc. Am. B* **25**, 1284 (2008).
- [27] W. Riley, *Handbook of Frequency Stability Analysis*, NIST Special Publication 1065 (National Institute of Standards and Technology, Gaithersburg, MD, 2008).
- [28] C. E. Calosso, C. Clivati, and S. Micalizio, [arXiv:1507.00458](https://arxiv.org/abs/1507.00458).
- [29] E. Benkler, C. Lisdat, and U. Sterr, *Metrologia* **52**, 565 (2015).
- [30] W.-K. Lee, D.-H. Yu, C. Y. Park, and J. Mun, *Metrologia* **47**, 24 (2010).
- [31] O. Lopez, A. Haboucha, F. Kéfélian, H. Jiang, B. Chanteau, V. Rocin, C. Chardonnet, A. Amy-Klein, and G. Santarelli, *Opt. Express* **18**, 16849 (2010).
- [32] T. R. Parker, M. Farhadiroushan, V. A. Handerek, and A. J. Rogers, *Opt. Lett.* **22**, 787 (1997).
- [33] T. J. Pinkert, O. Böll, G. S. M. Jansen, E. A. Dijk, B. G. H. M. Groeneveld, R. Smets, F. C. Bosveld, W. Ubachs, K. Jungmann, K. S. E. Eikema, and J. C. J. Koelemij, *Appl. Opt.* **54**, 728 (2015).
- [34] M. Hinkley, J. A. Sherman, N. B. Phillips, M. Schioppa, N. D. Lemke, K. Beloy, M. Pizzocaro, C. W. Oates, and A. D. Ludlow, *Science* **341**, 1215 (2013).